Jumping Further: Forward Jumps in a Gravity-reduced Immersive Virtual Environment

HyeongYeop Kang*
Computer Science Department
Korea University

Geonsun Lee†
Computer Science Department
Korea University

Dae Seok Kang‡
CT Convergence Group
KITECH

Ohung Kwon§
CT Convergence Group
KITECH

Jun Yeup Cho¶
Computer Science Department
Korea University

Ho-Jung Choi‖
CT Convergence Group
KITECH

JungHyun Han**
Computer Science Department
Korea University

ABSTRACT

In a cable-driven suspension system developed to simulate the reduced gravity of lunar or Martian surfaces, we propose to manipulate/reduce the physical cues of forward jumps so as to overcome the limited workspace problem. The physical cues should be manipulated in a way that the discrepancy from the visual cues provided through the HMD is not noticeable by users. We identified the extent to which forward jumps can be manipulated naturally. We combined it with visual gains, which can scale visual cues without being noticed by users. The test results obtained in a prototype application show that we can use both trajectory manipulation and visual gains to overcome the spatial limit. We also investigated the user experiences when making significantly high and far jumps. The results will be helpful in designing astronaut-training systems and various VR entertainment content.

Index Terms: Human-centered computing—Human computer interaction (HCI)—Interaction paradigms—Virtual reality; Human-centered computing—Human computer interaction (HCI)—HCI design and evaluation methods—User studies

1 INTRODUCTION

There has been an increasing demand for simulating the sensations of reduced gravity, which astronauts would experience in the lunar or Martian surfaces. We have developed a cable-driven system to simulate the reduced gravity on the earth. In the system, the cable composed of four wires lifts a user so that part of the user's weight is offloaded onto the cable. If $^5/_6$ of the weight is offloaded, for example, the user will have a sensation of being in lunar surface. When the motion platform is integrated with VR, however, it often suffers from the problem of the limited workspace, and locomotion in the VR motion platform may cause an accident of hitting its steel frame.

Focusing on the forward jump in the gravity-reduced environment, this paper proposes to manipulate the wires to reduce the physical trajectory whereas the visual cue provided through the HMD follows the original ballistic trajectory. Our goal is to manipulate the physical trajectory in a way that the discrepancy from the visual trajectory is not noticeable by users. An experiment was conducted for identifying the extent to which the jump can be manipulated naturally.

An additional experiment was made to estimate the range of visual gains, which scale the visual trajectory without being noticed by users. Then, we tested whether the trajectory manipulation and visual gains can be simultaneously used for extending the jumping distance and height. The test was performed in a prototype application, where users jump between buildings in a futuristic extraterrestrial metropolis. The results show that we can use both trajectory manipulation and visual gains to overcome the spatial limit of a VR motion platform. Lastly, user experiences were investigated between significantly high and far jumps. The results will be helpful in designing VR jump applications.

*e-mail: siamiz88@gmail.com
†e-mail: g_sun@korea.ac.kr
‡e-mail: kds60513@kitech.re.kr
§e-mail: ohung@kitech.re.kr
¶e-mail: abslon@korea.ac.kr
‖e-mail: ilovehjb0520@kitech.re.kr
**e-mail: jhan@korea.ac.kr

2 RELATED WORK

One of the primary goals in developing an immersive virtual environment (IVE) is to increase the sense of *presence*. According to the definition by Witmer and Singer [36], presence is a "subjective experience of being in one place even when physically situated in another.'' In order to intensify such sensation, many researchers suggested to provide multisensory cues [7, 33]. They may include the visual, somatosensory, auditory, and vestibular cues that immerse users in the virtual environment and enrich the overall experience. Several experiments investigated on how visual and vestibular cues contribute to users' self-motion perception [12, 37]. Wright et al. [37] pointed out that visual motion detectors are velocity sensitive whereas vestibular receptors are acceleration sensitive.

The vestibular cues are often reproduced by using motion simulators. They range from vehicle installations such as flight [1, 20] and driving simulators [17, 21, 22] to systems that directly operate on the user's limbs such as swimming [8], scuba diving [15], parachute [13, 31], and skydiving simulators [6].

Motion simulators are also useful to reproduce a gravity-reduced environment [3, 10, 35]. Fujii et al. [9] presented a suspension system which employs a weight counterbalancing method. Griffin [11] developed a water-based buoyancy pool that simulates the weightlessness. A 3DOF gravity-reduced simulator developed by Xiu et al. [39] adopted a spring-based passive static balancing technology to enable walking in an environment of micro/reduced gravity. Xiang et al. [38] proposed a suspension system that is based on passive static balancing technique and active dynamic servo technique. The system was composed of a force sensor, an electro servo winch, and a treadmill, and was tested on walking motions under simulated lunar gravity. NASA developed a cable-based suspension system, named ARGOS [5]. It was composed of a bulky complicated gantry and a large drum winch. Kim et al. [18] presented a suspension system, which provided similar functionalities as ARGOS but was built upon four wires.

A limitation of locomotion in IVEs is that a user cannot move through the virtual world that is larger than the workspace of the real

2019 IEEE Conference on Virtual Reality and
3D User Interfaces
23-27 March, Osaka, Japan
978-1-7281-1377-7/19/$31.00 ©2019 IEEE

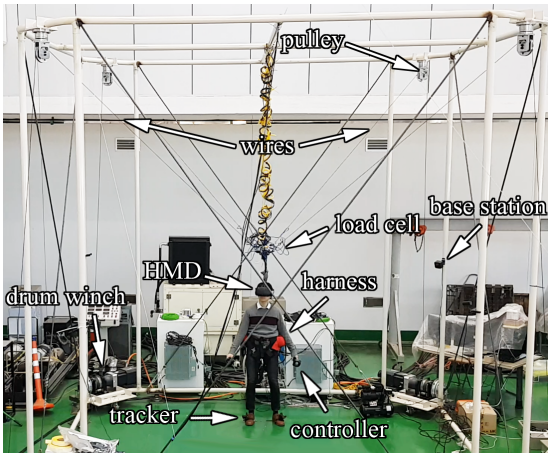

Figure 1: Cable-driven system for gravity-reduced virtual environment.

world. In the technique named *redirected walking* [28, 29, 34, 40], the user's locomotion is altered by a visual gain, which indicates the ratio of the movement in the virtual world to that in the real world, and is then displayed so that the virtual world moves differently from the real world. Unfortunately, an inadequate combination of visual and non-visual stimuli may cause a sensory conflict, often resulting in motion sickness [19, 25, 30]. To resolve this problem, numerous experiments were conducted to find the optimal visual gain range that combines the stimuli most naturally [14, 24, 27].

In the context of motion simulation, similar efforts have been made because the simulators also have a limited workspace, hence allowing constrained movements. The normally perceived visual gain ranges were investigated for users walking on a treadmill [24, 27]. Kang et al. [16] used a cable-driven system for a virtual parasailing application and found the naturally perceived visual gain range of the vertical flying movements.

Focusing on "jumping in place" on the virtual lunar surface, Kim et al. [18] identified how much the height of a jump could be scaled without being noticed by users. Their system provided constant gravitational acceleration of the virtual lunar surface, $g/6$, and altered the visual stimulus along the vertical direction only. In contrast, our system presented in this paper dynamically changes the horizontal/vertical accelerations of the forward jump and alters the visual stimulus not only vertically but also horizontally.

3 Gravity-Reduced Virtual Environment

Our motion platform for generating the reduced gravity is a cable-driven system shown in Fig. 1. Its dimensions are $4m \times 4m \times 4m$. It is equipped with four wires, each connecting a drum winch and the harness through a pulley. A drum winch with a 12KW motor can lift the harness up and down by pulling in or letting out the wire.

Our cable system has evolved over the years from a single wire to two and then four wires. For the current study on *forward jump*, the system restricts the user's motion to a sagittal plane, and four wires prevent unwanted sway motions quite effectively.

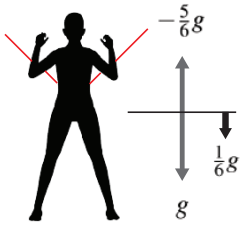

The gravitational acceleration on the earth surface is $9.8m/s^2$, and that on the lunar surface is $1/6$ of the earth's. If the tension of the cable is $5/6$ of a user's weight, the user will be provided with the lunar gravity, as depicted in the inset. A load cell located between a pulley and the harness senses its wire's tension, and the cable system can operate the motors of the winches so as to lift the user with a constant vertical force, which is $5/6$ of the user's weight.

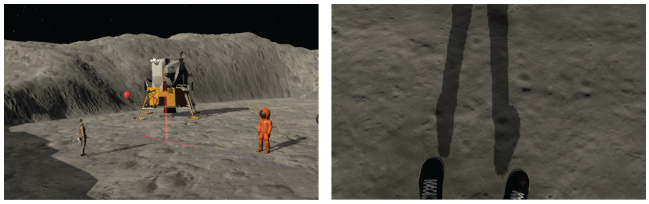

Figure 2: Scenes for the experiments: (a) The third person's view of the lunar surface. (b) The first person's view of the avatar's limbs and their shadows cast on the ground.

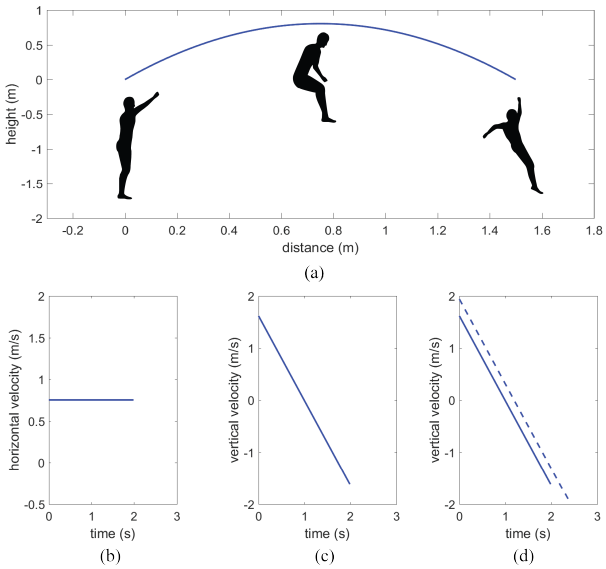

Figure 3: Trajectory and velocity of the forward jump: (a) The initial position of the junction is taken as $(0,0)$ in 2D. (b) The horizontal velocity remains constant. (c) The vertical velocity linearly decreases. (d) The solid line is copied from (c) whereas the dotted line is for an initial vertical velocity greater than (c).

Using HTC Vive headset, we set the tracking volume with "Room-scale mode." Its dimensions were about $3m \times 3m \times 3m$. A user's motion was tracked with three trackers and two wireless controllers. Two trackers were attached to both shoes and one was around the navel. The controllers were held in both hands. The tracked data was processed by the Unity game engine. All experiments were made on the lunar surface rendered by Unity, as shown in Fig. 2.

4 Forward Jump Manipulation

4.1 Forward Jump

The forward jump follows the principle of projectile motion illustrated in Fig. 3-(a), where the curve represents the trajectory of the junction of the harness and four wires. The trajectory is described in terms of horizontal distance (henceforth, simply 'distance') and height. It is determined by the initial velocity, which is decomposed into horizontal and vertical components. In our study, we assumed that the air resistance is negligible, making the horizontal velocity constant during the entire jumping motion. See Fig. 3-(b). In contrast, the vertical velocity linearly decreases due to the gravity, as shown in Fig. 3-(c). Consequently, the jumping trajectory in Fig. 3-(a) is symmetric.

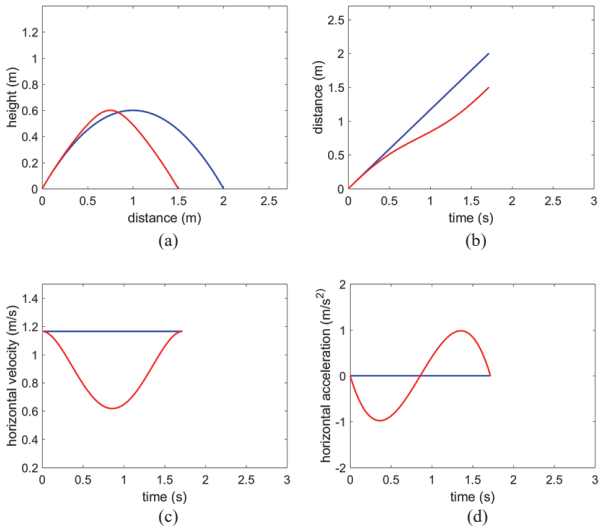

Figure 4: Horizontal manipulation: (a) Trajectory. (b) Horizontal $p(t)$. (c) Horizontal $\dot{p}(t)$. (d) Horizontal $\ddot{p}(t)$.

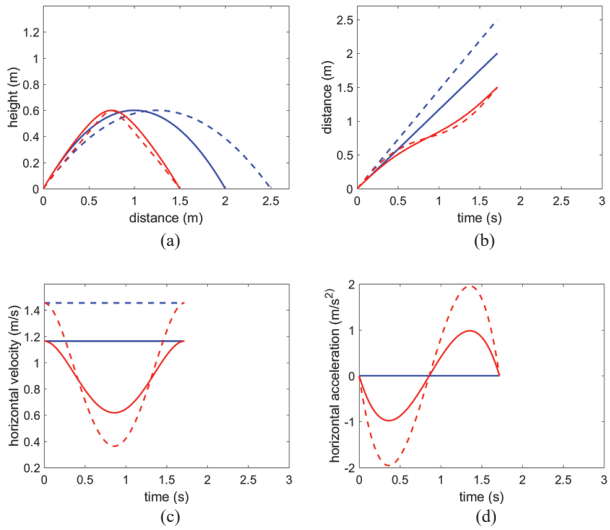

Figure 5: Comparison of horizontal manipulation: (a) Trajectories. (b) Horizontal $p(t)$. (c) Horizontal $\dot{p}(t)$. (d) Horizontal $\ddot{p}(t)$.

Suppose that a new jump is made with an initial vertical velocity greater than that of Fig. 3-(c). Due to the gravitational acceleration, the vertical velocity will be decreased with the same slope, as depicted in Fig. 3-(d). This shows that the duration of flight is proportional to the initial vertical velocity but is not affected by the horizontal velocity. Also note that the height of the forward-jump trajectory is determined only by the initial vertical velocity whereas the distance is determined by both horizontal and vertical velocities.

4.2 Limited Workspaces

The dimensions of our cable system are $4m \times 4m \times 4m$, but the actual workspace is reduced in order to avoid kinematic singularity and motor torque limit. There exist additional factors that further restrict the workspace. The tracking volume of HTC Vive is $3m \times 3m \times 3m$. The safe landing area should be secured because the final velocity at the time of landing is not zero and the user often moves ahead a bit further. Due to such many factors, the 'safe' distance is conservatively estimated to be $1.5m$ and the 'safe' height is $0.8m$. All forward jumps need to be physically confined to these ranges.

4.3 Horizontal Manipulation

Suppose that a user makes a forward jump. Once its initial velocity is measured, the expected distance and height of the forward jump can be immediately computed. If they exceed the pre-defined 'safe' ranges, they need to be *manipulated*, i.e., *reduced*. Fig. 4-(a) shows an example, where a $2m$-long forward jump (depicted in blue) is manipulated/reduced to the 'safe' distance, $1.5m$ (in red).

Let us first present how the horizontal motion of the forward jump is manipulated. The initial position is denoted as p_i, initial velocity as $\dot{p}_i$, and initial acceleration as $\ddot{p}_i$. The final position, velocity, and acceleration are denoted as p_f, $\dot{p}_f$, and $\ddot{p}_f$, respectively. At the time of takeoff, $\dot{p}_i$ is measured. As the horizontal motion is assumed to be made at a constant velocity, $\dot{p}_i = \dot{p}_f$ and $\ddot{p}_i = \ddot{p}_f = 0$. Whereas $p_i = 0$ by default, p_f is set to the desired 'safe' distance, $1.5m$ in the current study. Let t_f denote the duration of flight. Then, the distance at time t is defined as a quintic polynomial, which is widely used for trajectory generation in robotics and control systems [4]:

$$p(t) = \alpha_0 + \alpha_1 t + \alpha_2 t^2 + \alpha_3 t^3 + \alpha_4 t^4 + \alpha_5 t^5 \qquad (1)$$

where

$$\begin{aligned}
\alpha_0 &= p_i, \qquad \alpha_1 = \dot{p}_i, \qquad \alpha_2 = \frac{\ddot{p}_i}{2}, \\
\alpha_3 &= \frac{20p_f - 20p_i - (8\dot{p}_f + 12\dot{p}_i)t_f - (3\ddot{p}_i - \ddot{p}_f)t_f^2}{2t_f^3}, \\
\alpha_4 &= \frac{30p_i - 30p_f + (14\dot{p}_f + 16\dot{p}_i)t_f + (3\ddot{p}_i - 2\ddot{p}_f)t_f^2}{2t_f^4}, \\
\alpha_5 &= \frac{12p_f - 12p_i - (6\dot{p}_f + 6\dot{p}_i)t_f - (\ddot{p}_i - \ddot{p}_f)t_f^2}{2t_f^5}.
\end{aligned} \qquad (2)$$

The red curve in Fig. 4-(b) represents the distance, $p(t)$, for the manipulated jump. Note that it is not linear.

The first derivative of $p(t)$ defines the manipulated velocity, $\dot{p}(t)$. It is the red curve in Fig. 4-(c). The manipulated acceleration, $\ddot{p}(t)$, is illustrated in Fig. 4-(d). Whereas the negative acceleration implies that the wires pull the user backward, the positive acceleration implies that the wires push the user forward so as to make $\dot{p}_f$ equal to $\dot{p}_i$.

Fig. 5-(a) adds a $2.5m$-long jump (in dotted blue) to Fig. 4-(a). As depicted in the dotted-red curve, the trajectory is manipulated to be 'safe.' The rest of Fig. 5 show $p(t)$, $\dot{p}(t)$, and $\ddot{p}(t)$ for the manipulated $2.5m$-long jump.

4.4 Vertical Manipulation

Let us now consider the vertical motion of the forward jump. Fig. 6-(a) shows an example, where a $1m$-high jump (depicted in blue) is manipulated to the 'safe' height, $0.8m$ (in red). Equation (1) applies also to the vertical motion. In the *ascending* phase, (1) $p_i = 0$, (2) $\dot{p}_i$ is measured at the time of takeoff, (3) $\ddot{p}_i$ is fixed to the gravitational acceleration, i.e., $-g/6$ on the lunar surface, (4) p_f is set to the desired 'safe' height, $0.8m$, (5) $\dot{p}_f = 0$, and (6) $\ddot{p}_f$ remains $-g/6$. In the *descending* phase, (1) $p_i = 0.8m$, (2) $\dot{p}_i = 0$, (3) $\ddot{p}_i = -g/6$, (4) $p_f = 0$, (5) $\dot{p}_i$ of the ascending phase is negated to define $\dot{p}_f$, and (6) $\ddot{p}_f = -g/6$. Fig. 6-(b), -(c), and -(d) depict the height, vertical velocity, and vertical acceleration curves, respectively.

Fig. 7-(a) adds a $1.2m$-high jump (in dotted blue) to Fig. 6-(a). As depicted in the dotted-red curve, the trajectory is manipulated

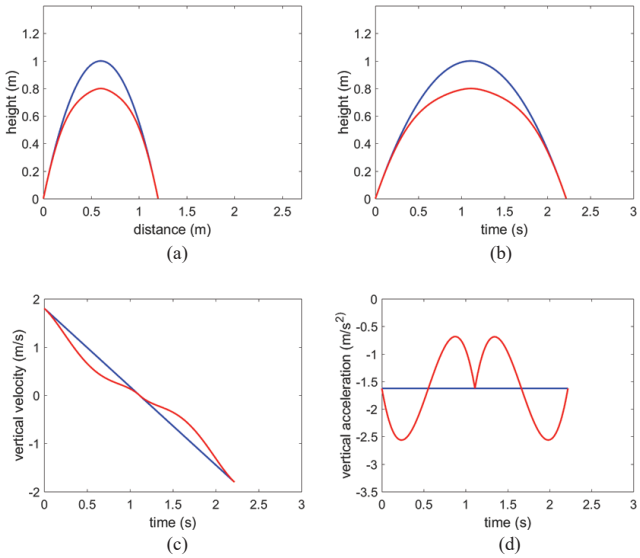

Figure 6: Vertical manipulation: (a) Trajectory. (b) Vertical $p(t)$. (c) Vertical $\dot{p}(t)$. (d) Vertical $\ddot{p}(t)$.

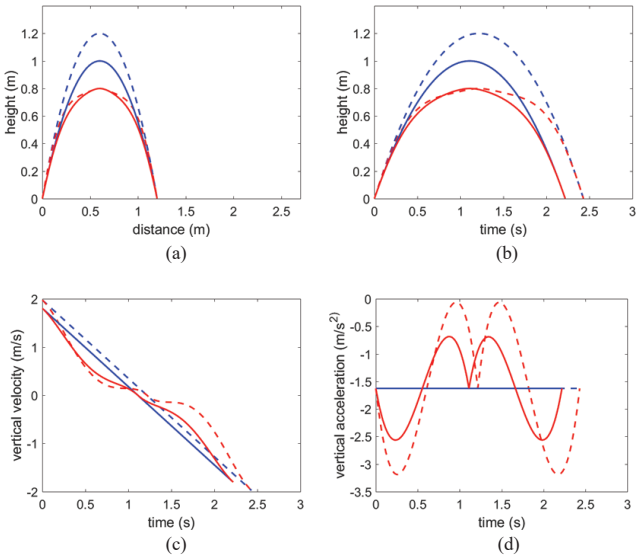

Figure 7: Comparison of vertical manipulation: (a) Trajectories. (b) Vertical $p(t)$. (c) Vertical $\dot{p}(t)$. (d) Vertical $\ddot{p}(t)$.

to be 'safe.' The rest of Fig. 7 show $p(t)$, $\dot{p}(t)$, and $\ddot{p}(t)$ for the manipulated $1.2m$-high jump. Note the change in the duration of flight.

4.5 Wire Control

As presented in Sections 4.3 and 4.4, $p(t)$, $\dot{p}(t)$, and $\ddot{p}(t)$ are computed for both horizontal and vertical directions. They are combined to define the 'manipulated' position, velocity, and acceleration of the junction (of the harness and four wires). On the other hand, the 'actual' position, velocity, and acceleration of the junction are obtained from the encoders embedded in the electric motors of the drum winches. The differences determine the position, velocity, and acceleration errors, which are denoted by e, $\dot{e}$, and $\ddot{e}$, respectively, and the overall force of the cable system required for manipulation is defined as follows:

$$f = k_1 mg + k_2 e + k_3 \dot{e} + k_4 \ddot{e} \tag{3}$$

where k_i represent the control gains and m is the user's mass.

The required force, f, is distributed to four wires through a kinematic transformation. Let f^i denote the force assigned to the i-th wire. Let τ^i denote the actual tension of the i-th wire, which is measured every 2 milliseconds by the load cell. Then, a tension proportional-integral-derivative (PID) controller determines the torque for driving the motor of the drum winch to wind up or let out the wire. It makes the tension error, $f^i - \tau^i$, zero. We do not suffer from the sensor-actuator latency because both sensing and actuation are made by the drum winches and the control period is 2 milliseconds.

4.6 Problem Definition

In Fig. 7-(a), the blue curves represent the *visual cue* provided through the HMD and the red curves represent the *physical cue* provided by the cable system. Whereas the visual-vestibular discrepancy between the dotted curves (for the $1.2m$-high jump) may be noticed by users, the discrepancy between the solid blue and red curves (for the $1m$-high jump) may not be noticed due to the smaller extent of manipulation. Similar discussions can be made for horizontal manipulation in Fig. 5-(a). Our goal is to manipulate the physical trajectory in a way that the discrepancy from the visual trajectory is not noticed by users. To this end, we need to identify the maximum allowable extent of manipulation.

Even if we build a larger cable system, we may still encounter the limited-workspace problem depending on applications, making it necessary to manipulate the trajectory. For example, consider developing a triple-jump application. It could not be secured even with a $6m \times 6m \times 6m$ cable system, and the three jumps need to be manipulated without being noticed by users.

5 Pilot Tests

Before designing the main experiments, we conducted pilot tests with eight volunteers (six males and two females) including the authors of this paper. They repeated the $1.5m$-long and $0.8m$-high 'safe' jump 10 times. For distances, the mean (μ) was 1.4966 and the standard deviation (σ) was 0.1408. The maximum distance error was about $0.15m$, i.e., the longest distance among 80 jumps (made by eight participants) was about $1.65m$. For heights, $\mu = 0.7745$, $\sigma = 0.0257$, and the maximum error was about $0.1m$.

The participants then made a pair of $1.65m$-long jumps, where one was reduced to the 'safe' distance, $1.5m$, and the other was not. It was repeated 10 times. Similarly, a pair of $0.9m$-high jumps were repeated 10 times, where one was reduced to the 'safe' height, $0.8m$, and the other was not. The jumps were presented in counter-balanced order. The post-test user survey showed that no participant could discriminate the manipulated jump from the normal one.

For every jump reported in this paper, the target distance and height were indicated in the virtual environment by displaying a line on the ground and a ball in the air, respectively. While jumping, the user could see their avatar's limbs and shadows cast on the ground, as shown in the video and Fig. 2-(b).

6 Experiment 1: Acceleration Thresholds

Our study comprised a primary experiment and a secondary one. The objective of the primary experiment (henceforth, E1) was to identify the maximum extent of manipulation that does not cause the visual-vestibular discrepancy. The vestibular organs do not respond to constant velocity but respond only to changes in velocity, i.e., acceleration [23]. Therefore the goal of E1 boils down to identifying the *acceleration thresholds* for trajectory manipulation. Since the

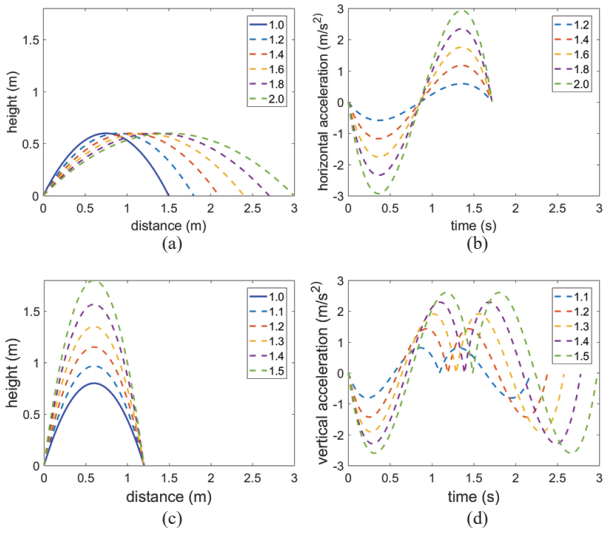

Figure 8: Jump manipulation: (a) Horizontal manipulation with the target height fixed to $0.6m$. (b) Accelerations required for the trajectories shown in (a). (c) Vertical manipulation with the target distance fixed to $1.2m$. (d) Accelerations required for the trajectories shown in (c).

acceleration threshold for vertical motion is different from that for horizontal motion [2], we identified them separately.

6.1 Participants

Seven (five males and two females) subjects participated in E1. Their ages were in the range of $[21,23]$ ($\mu = 22.42$, $\sigma = 0.53$), the heights (in cm) were in $[158,181]$ ($\mu = 172.71$, $\sigma = 7.25$), and the weights (in kg) were in $[51,100]$ ($\mu = 74.85$, $\sigma = 19.36$). All subjects had normal or corrected-to-normal vision, and six had experiences in HMD. All subjects signed an informed consent form, and the experiments were approved by the Korea University Institutional Review Board.

6.2 Method and Procedure

The horizontal and vertical motions were tested separately. For the horizontal test, the $1.5m$-long 'safe' jump was taken as a *reference*. Its distance was multiplied by 1.2, 1.4, 1.6, 1.8, and 2.0 to define five more jumps. (We call these numbers *multipliers*.) Fig. 8-(a) shows the trajectories of six jumps, where the dotted ones were manipulated to be $1.5m$ long. The cable system provided more control on the acceleration for a longer jump. Fig. 8-(b) shows the horizontal acceleration curves for the manipulated jumps.

For the vertical test, the $0.8m$-high 'safe' jump was taken as a reference. The initial vertical velocity to reach the peak of $0.8m$ was computed, and then it was multiplied by 1.1, 1.2, 1.3, 1.4, and 1.5 to define five more jumps. As the peak's height is proportional to the square of the initial vertical velocity, the target heights are $0.8m$, $0.97m$, $1.15m$, $1.35m$, $1.57m$, and $1.8m$. See Fig. 8-(c). The dotted trajectories were manipulated to be $0.8m$ high. Fig. 8-(d) shows the vertical acceleration curves for the manipulated jumps.

E1 began with 30-minute training. It was composed of (1) ten minutes of free jumping, (2) five minutes of jumping to uniformly-sampled target distances, (3) five minutes of jumping to uniformly-sampled target heights, and (4) ten minutes of jumping to arbitrarily-chosen distances and heights. With the 30-minute training, the subjects got used to the gravity-reduced environment and the trials made at (4) were by and large successful.

In the horizontal test, a block was composed of six jumps, each with a distinct distance, and a subject went through 12 blocks. The order of jumps was counter-balanced between blocks. In the same manner, a block in the vertical test was composed of six jumps, each with a distinct height, and a subject went through 12 blocks. After a jump was taken, the HMD screen faded out to black and the subject was asked to choose between 'manipulated' and 'natural.' A jump including the Q&A took about 20 seconds, and a two-minute break was between blocks. Right before and after each of the horizontal and vertical tests, the subject filled out the Simulator Sickness Questionnaire (SSQ).

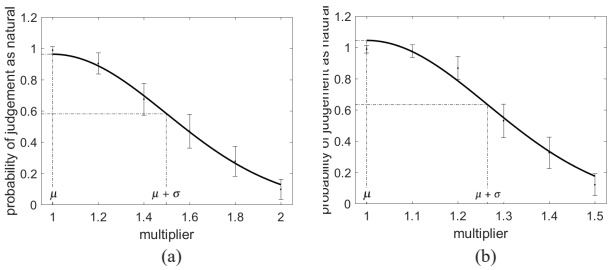

Figure 9: The experiment results of E1: (a) Horizontal manipulation. (b) Vertical manipulation.

6.3 Result and Discussion

In the horizontal test, the distance and height of the *reference jump* were $1.5m$ and $0.6m$, respectively. We pre-computed the *initial velocity* needed to reach the distance and height. Let us denote its horizontal component as $v_{r,h}$. On the other hand, consider the target distance defined by a multiplier $\mathbf{m}$. At the time of takeoff toward the target, the initial horizontal velocity, $v_{\mathbf{m},h}$, was measured. If $v_{\mathbf{m},h}/v_{r,h}$ was in the range of $[\mathbf{m}-0.1,\mathbf{m}+0.1]$, the jump was taken as valid. Otherwise, it was taken as invalid and discarded. (The window of width 0.2 was made equal to the multiplier's interval shown in Fig. 8-(a).) Out of 504 jumps made by all subjects, six (about 1.2%) were invalid.

In the vertical test, the validity of a jump was similarly assessed. Let $v_{r,v}$ denote the initial vertical velocity needed to reach the height, $0.8m$, of the reference jump and $v_{\mathbf{m},v}$ denote the initial vertical velocity measured at the time of takeoff toward a specific target height with a multiplier $\mathbf{m}$. The multiplier's interval for vertical manipulation is 0.1, as shown in Fig. 8-(c). If $v_{\mathbf{m},v}/v_{r,v}$ was not in the range of $[\mathbf{m}-0.05,\mathbf{m}+0.05]$, the jump was taken as invalid. Five out of 504 jumps (about 1.0%) were invalid.

The valid jumps were analyzed, and the results are illustrated in Fig. 9, where the x-axis is for the multiplier and the y-axis shows the probability of taking the manipulated jump as 'natural.' (The probability is the number of natural jumps divided by the total number of jumps.) The curves show the fitted Gaussian functions of the form $f(x) = \frac{a}{e^{-(x-1)^2/2b^2}}$ with real numbers a and b. In both horizontal and vertical directions, the multiplier of 1.0 is taken as the mean (μ) of Gaussian function, i.e., 1.0 is taken as the *most natural*. The *largest natural* multiplier is defined to be $\mu+\sigma$, where σ denotes the standard deviation.

Table 1: The ranges of natural multipliers obtained from Fig. 9. R^2 denotes the coefficient of determination.

direction	μ	σ	$\mu+\sigma$	R^2
horizontal	1.00	0.47	1.47	0.99
vertical	1.00	0.26	1.26	0.98

Table 1 shows that the largest natural multiplier for 'horizontal' manipulation is 1.47. Then, $p(t)$ given in Equation (1) is computed by taking $1.47v_{r,h}$ as $\dot{p}_i$ and using the assumptions that $p_i = 0$, $p_f =$

$1.5m$, $\dot{p}_i = \dot{p}_f$, and $\ddot{p}_i = \ddot{p}_f = 0$. The peak amplitude of its second derivative, $\ddot{p}(t)$, is $1.37m/s^2$. This is the *horizontal acceleration threshold*, i.e., the maximum horizontal acceleration which allows the manipulated jump to be perceived natural.

Table 1 shows that the largest natural multiplier for 'vertical' manipulation is 1.26. Taking $1.26v_{r,v}$ as $\dot{p}_i$, the peak amplitude of $\ddot{p}(t)$ is computed. It is $1.69m/s^2$, which represents the *vertical acceleration threshold*.

We investigated whether the repeated jumps affected the subjects' choices. In each of horizontal and vertical directions, we extracted the first six and last six blocks, and performed Wilcoxon signed-rank test. There were no significant differences between the two groups of blocks in both horizontal manipulation ($Z = -0.115, p > 0.05, r = 0.005$) and vertical manipulation ($Z = -0.500, p > 0.05, r = 0.02$). The two-minute break between every two consecutive blocks may have relieved the subjects of fatigue.

The pre- and post-SSQs were compared by Wilcoxon signed-rank test. The results showed that there were no significant differences in both horizontal manipulation ($Z = -0.577, p > 0.05, r = 0.15$) and vertical manipulation($Z = -1.414, p > 0.05, r = 0.38$).

7 Experiment 2: Visual Gains

It is well-known that visual cues dominate other multisensory cues [26]. Exploring such visual dominance, *visual gains* have been widely adopted in IVEs [24, 33]. A visual gain is defined as the ratio of the virtual-world displacement to the real-world one. Suppose that, for example, it is set to $4/3$ in our VR motion platform. Then, if a user makes a $1.5m$-long physical jump, the visual cue provided through the HMD will be a $2m$-long jump. If the user does not notice any discrepancy between the physical and visual cues, it implies that the user's perception is successfully deceived.

Our hypothesis is that such visual gains can be integrated with the trajectory manipulation discussed in the previous section. Suppose that, for example, the user's jump is pulled $0.5m$ backward by a cable system. If the user still perceives the jump to be natural, our system successfully gives the user the sensation of jumping $2m$ long while confining them to the $1m$ range. The cable system's virtual workspace is extended one level further.

The secondary experiment (henceforth, E2) was conducted to estimate the range of *visual gains*, which scale the visual cue without having the user perceive any discrepancy. As will be presented in Section 8, both trajectory manipulation and visual gains can be simultaneously used to extend the distance and height of a forward jump.

7.1 Participants

In E2, seven subjects (four males and three females) participated. Five subjects were re-recruited from E1, but they took E2 a week after to prevent from getting used to the gravity-reduced environment. The ages of the subjects were in the range of $[20, 25]$ ($\mu = 22.57$, $\sigma = 1.51$), the heights (in cm) were in $[158, 175]$ ($\mu = 168.57$, $\sigma = 7.43$), and the weights (in kg) were in $[51, 98]$ ($\mu = 67.14$, $\sigma = 17.17$). All subjects had normal or corrected-to-normal vision, and five had experiences in HMD.

7.2 Method and Procedure

As in E1, the horizontal and vertical motions were tested separately. Unlike E1, however, E2 instructed each subject to repeat the *reference jump*. For the horizontal movement, it was $1.5m$ long and $0.6m$ high. The reference jump was not manipulated at all, but the visual gain, denoted as g_v, was applied to the distance. It was in the range of $[0.6, 1.8]$ with steps of 0.2. When $g_v = 1$, i.e., when the physical and virtual jumps are identical, we say that the user is given the *standard stimulus*. In contrast, the user is provided with a *test stimulus* if $g_v \neq 1$. Fig. 10-(a) illustrates the standard stimulus (solid curve) and six test stimuli.

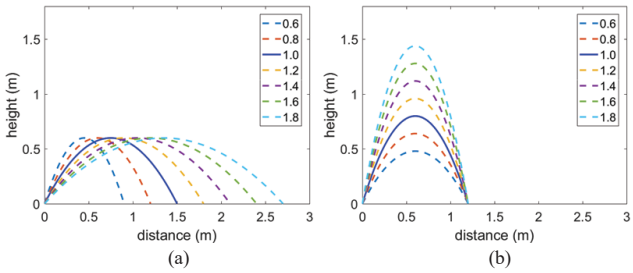

Figure 10: Gain-applied trajectories: (a) Horizontal visual gains. (b) Vertical visual gains.

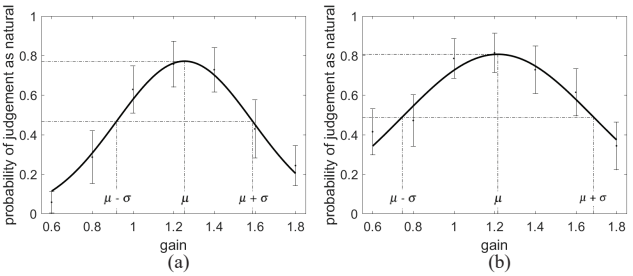

Figure 11: The experiment results of E2: (a) Horizontal direction. (b) Vertical direction.

For the vertical movement, the reference jump was $1.2m$ long and $0.8m$ high. To the height, we applied the same visual gains used in the horizontal movement, i.e., g_v in the range of $[0.6, 1.8]$ with steps of 0.2. See Fig. 10-(b).

E2 began with 20-minute training. It was partitioned into 5-minute free jumps "without wearing the HMD" and 15-minute jumps "with the HMD." The latter was composed of 5 minutes of free jumps, 5 minutes of the 'horizontal' reference jump, and 5 minutes of the 'vertical' reference jump.

In the main test for the horizontal movement, a block was composed of 10 jumps. The first three were the standard stimuli, and the remaining seven were randomly ordered test stimuli, each with a distinct value of g_v. Each subject was tested with 10 blocks, taking 100 jumps in total. The order of the test stimuli was counter-balanced between blocks. In the same manner, a subject took 100 jumps for the vertical movement. After each test-stimulus jump, the subject was asked to choose whether the perceived speed of the virtual jump was 'too fast,' 'natural,' or 'too slow' compared to the physical jump.

7.3 Result and Discussion

In the horizontal movement, the 'valid' ranges were set to $[1.35m, 1.65m]$ for distance and $[0.5m, 0.7m]$ for height. (The window widths, 0.3 and 0.2, were based on the results of the pilot tests presented in Section 5.) Out of 490 jumps, eleven (about 2.2%) were invalid and excluded from analysis. In the vertical movement, the valid ranges were $[1.05m, 1.35m]$ for distance and $[0.7m, 0.9m]$ for height. Nine out of 490 jumps (about 1.8%) were invalid and excluded.

Fig. 11 shows the analysis results. The x-axis is for the visual gain and the y-axis shows the probability that the gain-applied jump is judged as natural. The curves are Gaussian functions of the form $f(x) = \frac{a}{e^{-(x-b)^2/2c^2}}$ with real numbers a, b, and c. See Table 2 for μ and σ: μ is taken as the most natural gain, and the range of natural gains is defined by $\mu \pm \sigma$.

Table 2: The ranges of natural gains obtained from Fig. 11. R^2 denotes the coefficient of determination.

direction	μ	σ	$\mu \pm \sigma$	R^2
horizontal	1.25	0.33	[0.92, 1.58]	0.99
vertical	1.22	0.47	[0.75, 1.69]	0.96

Wilcoxon signed-rank test showed that there was a significant difference between the distributions of natural gains in the horizontal and vertical directions ($Z = -5.074, p < 0.05, r = 0.16$). We also tested whether the repeated jumps affected the subjects' choices. For the horizontal direction, the first five and last five blocks were extracted and compared by Wilcoxon signed-rank test. The same comparison was made for the vertical direction. The test results showed that there were no significant differences between the early and late phases in both horizontal ($Z = -1.554, p > 0.05, r = 0.07$) and vertical ($Z = -1.692, p > 0.05, r = 0.08$) directions.

The responses to the SSQ were also analyzed by Wilcoxon signed-rank test, and the result showed that there were no significant differences in both horizontal ($Z = -1.000, p > 0.05, r = 0.27$) and vertical ($Z = -1.414, p > 0.05, r = 0.38$) directions.

8 Test 1

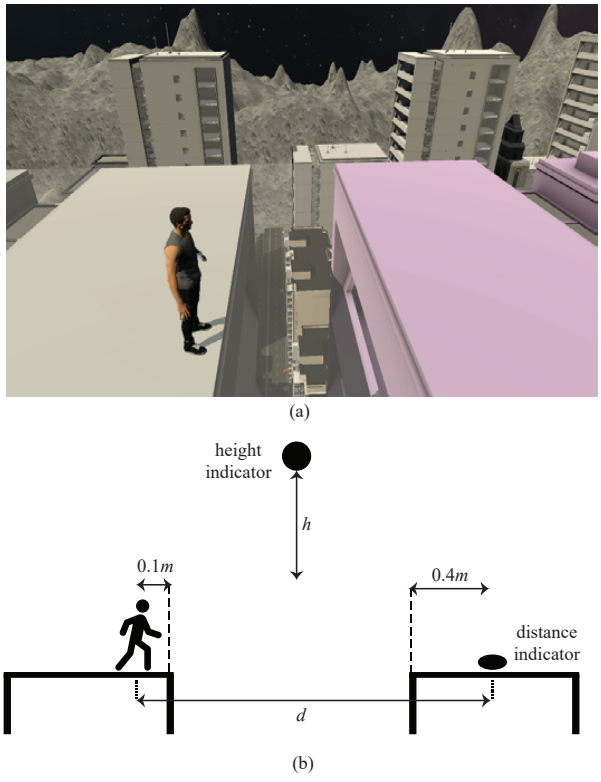

Figure 12: Jumping between buildings: (a) A translucent glass floor is provided between buildings to reduce the user's fear. (b) The distance/height indicators guide the user's jump.

We developed a test (henceforth, T1), where we combined the acceleration thresholds (obtained in E1) and allowable visual gains (obtained in E2) to measure the *sense of presence*. We recruited seven volunteers (five males and two females) for T1. Three subjects were re-recruited from E2, but E2 and T1 were separated by a week.

In T1, users jumped between buildings in a futuristic extraterrestrial metropolis (Fig. 12-(a)). The participants had free-jump training

Table 3: Four test cases in T1, where d means target distance and h means target height.

test cases	d	h	horizontal g_v	vertical g_v
case 1	1.80m	0.90m	1.00	1.00
case 2	3.10m	1.27m	1.00	1.00
case 3	1.80m	0.90m	1.25	1.22
case 4	3.10m	1.27m	1.25	1.22

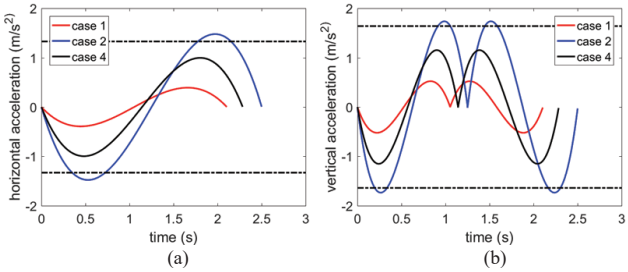

Figure 13: Acceleration curves in **cases 1**, **2**, and **4** listed in Table 3 and the acceleration thresholds (in dotted lines) identified in E1: (a) Horizontal accelerations. (b) Vertical accelerations.

for 15 minutes and then moved to the main test composed of four cases presented in Table 3. In each case, the participants first of all had 10-minute training of the gain-applied jumps, where the target distance and height were arbitrarily given within the 'safe' ranges. Then, with the case-specific distance (d) and height (h) designated by the indicators (Fig. 12-(b)), the participants made 10 consecutive jumps. A 20-minute break was between cases. Our hypotheses for the cases were as follows:

- **case 1**: Given d ($= 1.80m$) and h ($= 0.90m$), we can compute $\ddot{p}(t)$ for both horizontal and vertical trajectory manipulation, as presented in Sections 4.3 and 4.4. In Fig. 13, the curves of $\ddot{p}(t)$ are depicted in red. The peak amplitudes are smaller than the acceleration thresholds (in dotted lines) identified in E1, and therefore the manipulation may not be noticed.
- **case 2**: As was done in **case 1**, we can compute $\ddot{p}(t)$. In Fig. 13, the curves of $\ddot{p}(t)$ are depicted in blue. The peak amplitudes are larger than the acceleration thresholds, and therefore the manipulation may be noticed.
- **case 3**: Unlike **case 1** and **case 2**, the visual gains are not 1.00 but 1.25 and 1.22, which are the *most natural* gains presented in Table 2. Dividing d ($= 1.80m$) by 1.25 results in $1.44m$. Whereas the cable system translates a user by $1.44m$, the visual cue provided through the HMD translates the user by $1.80m$. The 10-minute 'per-case' training will make the participants get used to such a gain-applied jump. As $1.44m$ is within the 'safe' range, no horizontal manipulation is required. The same discussion can be made for the vertical direction.
- **case 4**: Dividing d ($= 3.10m$) by 1.25 results in $2.48m$. It is not within the 'safe' range and therefore is manipulated. As was done in **case 1** and **case 2**, we can compute $\ddot{p}(t)$ to manipulate the $2.48m$-long jump. See the black curve in Fig. 13-(a). Its peak amplitude is smaller than the acceleration threshold, and therefore the manipulation may not be noticed. The same discussion can be made for the vertical direction.

After completing each case, the participants filled out Igroup Presence Questionnaire (IPQ) [32] with 7-point Likert scale responses. The IPQ analysis shows the sense of presence in terms of four factors: Spatial Presence (SP) related to the sense of being physically present in IVEs, Involvement (INV) that measures the attention devoted to IVEs, Experienced Realism (REAL) that estimates the

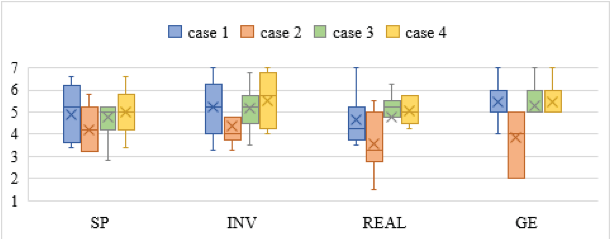

Figure 14: IPQ results in T1. Shown are the median, mean, interquartile ranges, and maximum/minimum values (whiskers).

subjective experience of realism in IVEs, and General Presence (GE) that assesses the general sense of being there. The analysis results are depicted in Fig. 14.

As hypothesized, **case 2** had the lowest scores in all factors. The trajectory manipulation was noticeable by users and decreased the sense of presence. In contrast, people tended to give the highest scores to **case 4** which has the same distance/height targets as **case 2**. This implies that we can use both trajectory manipulation and visual gains to overcome the spatial limit.

9 Test 2

In T1, some participants explicitly commented that **case 4** was more exciting than **case 1** and **case 3** because they were able to make a longer and higher jump. Inspired by this feedback, we designed another test (henceforth, T2) to investigate the relation between the distance/height of the forward jump and user experiences. T2 was conducted in the same environment as T1 (Fig. 12-(a)). We newly recruited eleven volunteers (ten males and one female) for T2.

Table 4: Three test cases in T2.

test cases	d	h	horizontal g_v	vertical g_v
standard	$2.00m$	$1.00m$	1.25	1.22
higher	$2.00m$	$1.50m$	1.25	1.22
longer	$3.00m$	$1.00m$	1.25	1.22

Table 4 lists three test cases. In every case, d and h divided by the visual gains are not 'safe' and are manipulated to $1.5m$ and $0.8m$, respectively. For each case, the participants had 10-minute training and then made 5 consecutive jumps. The cases were presented in counter-balanced order between participants. When completing a case, participants filled out the E^{2}I questionnaire [22] for investigating *presence* and *enjoyment*, and our own questionnaires. After completing three cases, participants were asked to choose the most exciting one out of three cases.

Table 5: E^{2}I analysis in T2.

test cases	presence		enjoyment	
	μ	σ	μ	σ
standard	43.45	4.82	24.55	4.59
higher	42.27	2.76	23.55	3.93
longer	46.73	3.72	27.64	2.69

The results of analyzing E^{2}I subscales are listed in Table 5, where **longer** scored the highest in both subscales. A one-way ANOVA test found that there were significant differences between the cases in terms of presence ($F(2,30) = 3.930, p < 0.05, \eta^2 = 0.21$) and enjoyment ($F(2,30) = 3.427, p < 0.05, \eta^2 = 0.19$). The post hoc comparisons using the Tukey's HSD test revealed that there were significant differences between **higher** and **longer** in both subscales.

Table 6: Our own questionnaires in T2 (No is 1, and Yes is 5).

questionnaire	standard		higher		longer	
	μ	σ	μ	σ	μ	σ
Q1. Were you able to land stably?	3.55	1.13	2.82	1.08	4.27	0.79
Q2. Was the jump easy to perform?	3.36	1.21	2.73	1.42	3.64	1.20
Q3. Was your jump natural?	4.00	0.63	3.91	0.54	4.45	0.52

Table 6 shows the analysis results of our own questionnaires. A one-way ANOVA test in Q1 found that there were significant differences between three cases ($F(2,30) = 5.714, p < 0.05, \eta^2 = 0.28$). The post hoc comparisons revealed that there was a significant difference between **higher** and **longer**. In contrast, we found that there were no significant differences between the cases in Q2 ($F(2,30) = 1.458, p > 0.05, \eta^2 = 0.09$) and Q3 ($X^2(2) = 4.880, p > 0.05, W = 0.07$) through a one-way ANOVA and Friedman tests respectively. It is notable that **higher** was taken as the most difficult, giving **higher** the lowest score in Q2. In an open-ended interview, three participants expressed anxiety when conducting **higher**. Lastly, when asked which jump was the most exciting, five participants chose **longer**, four chose **standard**, one chose **higher**, and one could not choose among the three.

10 Conclusion

We presented forward jumps in a gravity-reduced virtual environment, where the visual cue was provided through a VR headset and the physical cue was given by a cable-driven system. In order to provide unrestricted free jumps while the workspace was fairly restricted, we proposed to manipulate the physical trajectory and optionally apply visual gains to the visual trajectory. We identified how much the physical trajectory can be manipulated and how much visual gain can be applied without users' noticing.

Our study can be utilized for astronaut training, rehabilitation, and various VR applications such as skydiving and bungee jumping. Depending on applications, however, more study may often be needed. Note that we studied jumps in a flatland. Consider jumping down to a lower ground. If the height difference between the initial and final positions is larger, e.g., in jumping down to the ground from a $10m$ tall building, the final velocity to be used as a parameter of the quintic polynomial presented in Equation (1) could become much higher than people can tolerate. If the extensions can be made to accommodate such a velocity, however, we can provide diverse experiences such as heroes jump from the skyscraper and jumping down to the craters in the extraterrestrial planets.

The participants in the experiments provided insightful comments on the system. Many participants complained that it was time-consuming to wear the trackers and harness before mounting on the cable system. Several participants said that the longer the experiment went on, the more uncomfortable the harness became. These problems need to be addressed properly for practical uses in the future.

The goal of our study was to prevent the sense of discrepancy between physical and virtual jumps. However, such a discrepancy would be acceptable in VR fantasy games. Then it will be worth investigating how increasing discrepancy affects the user experiences. With the range of discrepancy in which user experiences remain acceptable, we can make a forward jump fairly longer and higher, and various VR fantasy games can be built upon the exaggerated jumps. Our future work will be done along the aforementioned directions.

Acknowledgments

This work was supported by the National Research Foundation of Korea (NRF) Grant funded by the Korea government (MSIT) (NRF-2017M3C4A7066316 and No. NRF2016-R1A2B3014319).

REFERENCES

[1] D. Allerton. *Principles of flight simulation*. John Wiley & Sons, 2009.

[2] A. Benson, M. Spencer, and J. Stott. Thresholds for the detection of the direction of whole-body, linear movement in the horizontal plane. *Aviation, space, and environmental medicine*, 1986.

[3] C. R. Carignan and D. L. Akin. Actively controlled mock-ups for eva training in neutral buoyancy. In *Systems, Man, and Cybernetics, 1997. Computational Cybernetics and Simulation., 1997 IEEE International Conference on*, vol. 3, pp. 2369–2374. IEEE, 1997.

[4] J. J. Craig. *Introduction to robotics: mechanics and control*, vol. 3. Pearson/Prentice Hall Upper Saddle River, NJ, USA:, 2005.

[5] T. Cunningham. System requirements document for the active response gravity offload system (argos). *NASA Engineering directorate document AR&SD-08007*, 2010.

[6] H. Eidenberger and A. Mossel. Indoor skydiving in immersive virtual reality with embedded storytelling. In *Proceedings of the 21st ACM Symposium on Virtual Reality Software and Technology*, pp. 9–12. ACM, 2015.

[7] L. Evans. Speed estimation from a moving automobile. *Ergonomics*, 13(2):219–230, 1970.

[8] S. Fels, Y. Kinoshita, T.-P. G. Chen, Y. Takama, S. Yohanan, A. Gadd, S. Takahashi, and K. Funahashi. Swimming across the pacific: a vr swimming interface. *IEEE Computer Graphics and Applications*, 25(1):24–31, 2005.

[9] H. Fujii, K. Uchiyama, H. Yoneoka, and T. Maruyama. Ground-based simulation of space manipulators using test bed with suspension system. *Journal of guidance, control, and dynamics*, 19(5):985–991, 1996.

[10] M. Glauser, Z. Lin, and P. E. Allaire. Modeling and control of a partial body weight support system: an output regulation approach. *IEEE Transactions on Control Systems Technology*, 18(2):480–490, 2010.

[11] B. Griffin. Zero-g simulation verifies eva servicing of space station modules. In *Space Station in the 21st Century*, p. 2312. 1986.

[12] L. R. Harris, M. Jenkin, D. Zikovitz, F. Redlick, P. Jaekl, U. Jasiobedzka, H. Jenkin, and R. S. Allison. Simulating self-motion i: Cues for the perception of motion. *Virtual Reality*, 6(2):75–85, 2002.

[13] J. Hogue, R. Allen, J. MacDonald, C. Schmucker, S. Markham, and A. Harmsen. Virtual reality parachute simulation for training and mission rehearsal. In *16th AIAA Aerodynamic Decelerator Systems Technology Conference and Seminar*, p. 2061, 2001.

[14] P. Jaekl, M. Jenkin, and L. R. Harris. Perceiving a stable world during active rotational and translational head movements. *Experimental brain research*, 163(3):388–399, 2005.

[15] D. Jain, M. Sra, J. Guo, R. Marques, R. Wu, J. Chiu, and C. Schmandt. Immersive terrestrial scuba diving using virtual reality. In *Proceedings of the 2016 CHI Conference Extended Abstracts on Human Factors in Computing Systems*, pp. 1563–1569. ACM, 2016.

[16] H. Kang, G. Lee, S. Kwon, O. Kwon, S. Kim, and J. Han. Flotation simulation in a cable-driven virtual environment–a study with parasailing. In *Proceedings of the 2018 CHI Conference on Human Factors in Computing Systems*, p. 632. ACM, 2018.

[17] N. Kaptein, J. Theeuwes, and R. Van Der Horst. Driving simulator validity: Some considerations. *Transportation Research Record: Journal of the Transportation Research Board*, (1550):30–36, 1996.

[18] M. Kim, S. Cho, T. Q. Tran, S.-P. Kim, O. Kwon, and J. Han. Scaled jump in gravity-reduced virtual environments. *IEEE Transactions on Visualization & Computer Graphics*, (4):1360–1368, 2017.

[19] E. M. Kolasinski. Simulator sickness in virtual environments. Technical report, ARMY RESEARCH INST FOR THE BEHAVIORAL AND SOCIAL SCIENCES ALEXANDRIA VA, 1995.

[20] W. J. Lam and L. De Vries. Flight simulator, Aug. 16 1983. US Patent 4,398,889.

[21] W.-S. Lee, J.-H. Kim, and J.-H. Cho. A driving simulator as a virtual reality tool. In *Robotics and Automation, 1998. Proceedings. 1998 IEEE International Conference on*, vol. 1, pp. 71–76. IEEE, 1998.

[22] J.-W. Lin, H. B.-L. Duh, D. E. Parker, H. Abi-Rached, and T. A. Furness. Effects of field of view on presence, enjoyment, memory, and simulator sickness in a virtual environment. In *Virtual Reality, 2002. Proceedings. IEEE*, pp. 164–171. IEEE, 2002.

[23] G. Mather. *Foundations of perception*. Taylor & Francis, 2006.

[24] N. C. Nilsson, S. Serafin, and R. Nordahl. Establishing the range of perceptually natural visual walking speeds for virtual walking-in-place locomotion. *IEEE transactions on visualization and computer graphics*, 20(4):569–578, 2014.

[25] C. M. Oman. Motion sickness: a synthesis and evaluation of the sensory conflict theory. *Canadian journal of physiology and pharmacology*, 68(2):294–303, 1990.

[26] M. I. Posner, M. J. Nissen, and R. M. Klein. Visual dominance: an information-processing account of its origins and significance. *Psychological review*, 83(2):157, 1976.

[27] W. Powell, B. Stevens, S. Hand, and M. Simmonds. Blurring the boundaries: The perception of visual gain in treadmill-mediated virtual environments. In *3rd IEEE VR 2011 Workshop on Perceptual Illusions in Virtual Environments*, 2011.

[28] S. Razzaque, Z. Kohn, and M. C. Whitton. Redirected walking. In *Proceedings of EUROGRAPHICS*, vol. 9, pp. 105–106. Citeseer, 2001.

[29] S. Razzaque, D. Swapp, M. Slater, M. C. Whitton, and A. Steed. Redirected walking in place. In *EGVE*, vol. 2, pp. 123–130, 2002.

[30] J. T. Reason. Motion sickness adaptation: a neural mismatch model. *Journal of the Royal Society of Medicine*, 71(11):819, 1978.

[31] M. Rheiner. Birdly an attempt to fly. In *ACM SIGGRAPH 2014 Emerging Technologies*, p. 3. ACM, 2014.

[32] T. Schubert, F. Friedmann, and H. Regenbrecht. The experience of presence: Factor analytic insights. *Presence: Teleoperators & Virtual Environments*, 10(3):266–281, 2001.

[33] G. Semb. Scaling automobile speed. *Perception & Psychophysics*, 5(2):97–101, 1969.

[34] F. Steinicke, G. Bruder, J. Jerald, H. Frenz, and M. Lappe. Estimation of detection thresholds for redirected walking techniques. *IEEE transactions on visualization and computer graphics*, 16(1):17–27, 2010.

[35] P. L. Swaim, C. J. Thompson, and P. D. Campbell. The charlotte (tm) intra-vehicular robot. 1994.

[36] B. G. Witmer and M. J. Singer. Measuring presence in virtual environments: A presence questionnaire. *Presence*, 7(3):225–240, 1998.

[37] W. Wright, P. DiZio, and J. Lackner. Vertical linear self-motion perception during visual and inertial motion: more than weighted summation of sensory inputs. *Journal of Vestibular Research*, 15(4):185–195, 2005.

[38] S. Xiang, H. Gao, Z. Liu, H. Yu, and Z. Deng. A novel active suspension gravity compensation system for physically simulating human walking in microgravity. In *Robotics and Biomimetics (ROBIO), 2016 IEEE International Conference on*, pp. 1052–1057. IEEE, 2016.

[39] W. Xiu, K. Ruble, and O. Ma. A reduced-gravity simulator for physically simulating human walking in microgravity or reduced-gravity environment. In *Robotics and Automation (ICRA), 2014 IEEE International Conference on*, pp. 4837–4843. IEEE, 2014.

[40] R. Zhang and S. A. Kuhl. Human sensitivity to dynamic rotation gains in head-mounted displays. In *Proceedings of the ACM Symposium on Applied Perception*, pp. 71–74. ACM, 2013.